JOURNAL OF GEOPHYSICAL RESEARCH, VOL. 106, NO. D24, PAGES 34,047–34,058, DECEMBER 27, 2001

Greenland ice sheet response to external forcing

C. J. van der Veen

Byrd Polar Research Center, Department of Geography, The Ohio State University, Columbus, Ohio

Abstract. Kinematic wave modeling is used to evaluate possible responses of the Greenland ice sheet to changes in its surface mass balance. In the approach followed here the reference state is defined based on measured velocity and discharge flux along the central flow line of Petermann Glacier in the northwest, and perturbations on this state are considered. The results indicate that significant rates of thickness change can occur immediately after the prescribed change in surface mass balance but adjustments in flow rapidly diminish these rates to a few centimeters per year at most. Full adjustment of the ice sheet requires times of the order of 1000 years. The instability mechanism known as the Jakobshavn Effect is discussed and, based on observational evidence as well as results from prior modeling studies, it is concluded that this is an unlikely mechanism for destabilizing major drainage basins of the Greenland ice sheet.

1. Introduction

One important finding that has come out of the concerted Program for Arctic Regional Climate Assessment investigations is that parts of the Greenland ice sheet are currently undergoing dramatic change. Applying the conventional method of comparing net input at the surface averaged over the period 1971-1990 (R. C. Bales et al., Accumulation map for the Greenland Ice Sheet, 1971-1990, submitted to *Geophysical Research Letters*, 2001) to discharge through exit gates circumnavigating the ice sheet close to the 2000 m elevation contour, *Thomas et al.* [2000] find a complex pattern of thickness change across the ice sheet, with the south-eastern sector thinning at a rate up to 30 cm yr^{-1}, while in the southwestern sector, thickening rates peak at 21 cm yr^{-1}. In the northern regions of the ice sheet, rates of thickness change are considerably less, with an average increase in ice thickness of 2 cm yr^{-1} in the northeast and thinning of 5 cm yr^{-1} in the northwest. Even greater rates of thickness change have been inferred for the lower reaches of several outlet glaciers which appear to be thinning at rates up to several meters per year [*Krabill et al.*, 1999]. These last results are based on repeat airborne laser profiling of the snow surface over a 5-year period, so the longer-term implications are not immediately obvious.

It may be that these large changes observed over a comparatively short time interval are a temporary manifestation of a change in the dynamic flow regime of these glaciers, for example, a short-lived surge. *Joughin et al.* [1996] report on a mini-surge on Ryder Glacier, north Greenland, during which the speed increased about threefold over a 7-week period. These authors suggest that the rapid motion, which occurred near the end of the 1995 ablation season, may have been caused by drainage of supraglacial lakes. Similarly, *Reeh and Oleson* [1986] measured velocity fluctuations of 10-15% on time scales from 2-10 days on Daugaard-Jensen Glacier, including an event corresponding to the drainage of an ice-dammed lake which caused a velocity increase of more than 50% over 12-18 hours. *Weidick* [1988] describes occurrences of surging in 26 locations in east Greenland between Daugaard-Jensen and Kangerdlugssuaq glaciers. While for none of these events measurements of the rate of thickness change are available, observations on other surging glaciers indicate that elevation changes up to several tens of meters per year are common during the active surge phase [*Van der Veen*, 1999a, section 10.4].

On the other hand, large thinning rates may reflect a more sustained switch in style of flow, in which case longer-term implications could be severe in terms of global sea level. The ice sheet may be reacting to recent changes in climate forcing, most notably to changes in the surface mass balance (snow accumulation minus ablation), or the current mass imbalance may be associated with the climate warming at the end of the Last Glacial Maximum (LGM), as temperature forcing results in a delayed ice sheet response. *Huybrechts* [1994] argues that current marginal thinning is likely due to increased surface melting caused by warmer temperatures following the Little Ice Age, while present-day thinning in the accumulation region of the Greenland ice sheet may be due to a slow but consistent warming of the basal ice following the warming after the LGM [*Whillans*, 1981].

A third possibility for observed imbalances may be that thinning of outlet glaciers is caused by increased creep rates, possibly associated with decreased basal friction as surface meltwater penetrates to the glacier bed [*Krabill et al.*, 1999]. *Hughes* [1986, 1998] argues that rapid ice discharge on outlet glaciers may be the manifestation of the Jakobshavn Effect, a powerful instability mechanism whereby small perturbations at the grounding line are amplified through the positive feedback between surface crevassing and meltwater penetration, extending creep flow, and progressive basal uncoupling. Ultimately, this feedback could possibly lead to the collapse of parts of the ice sheet.

Given the range of possible forcing mechanisms that may lead to important changes in the ice sheet, it is imperative to gain understanding of how each affects ice flow and drainage of interior ice. Without such understanding, predictions about the future evolution of the Greenland ice sheet cannot have much credibility.

Several approaches can be taken to evaluate the interaction between climate forcing and ice dynamics, and the consequent ice sheet response, which may involve changes in flow style. One possibility is to construct a time-evolving numerical model

Copyright 2001 by the American Geophysical Union.

Paper number 2001JD900032.
0148-0227/01/2001JD900032$09.00

in which the coupled thermomechanical equations of motion and conservation of energy are solved simultaneously. The major impediment to successfully constructing such a model is the paucity of data that can be used to first calibrate and then validate the model [*Van der Veen*, 1999b]. For many of the outlet glaciers draining the Greenland ice sheet, measurements of ice velocity are not available, thus making it impossible to identify and describe their flow regime and identify mechanical controls on glacier motion. Without full understanding of the current dynamics of the most active parts of the Greenland ice sheet, any numerical model employed in studies of the ice sheet's response to external forcings must invoke assumptions about the nature of ice discharge. The most common assumption is that of lamellar flow, in which the driving stress, responsible for glacier motion, is balanced by drag at the glacier bed. Making that assumption results in a rather sluggish ice sheet that reacts slowly to climate forcings. By allowing for basal sliding, the response may become more rapid but instabilities, such as the Jakobshavn Effect [*Hughes*, 1986], are unlikely to occur in these models in response to climate forcing. Indeed, on short timescales ice flow adjustments following a change in surface accumulation have little effect on the ice sheet evolution [*Huybrechts et al.*, 1991]. This suggests a more modest approach involving perturbation analysis as an alternative to full-scale modeling of the ice. That is, the assumption is made that the ice sheet response to mass balance forcing can be considered a perturbation on the reference state and may be evaluated separately from how this reference state evolves over time.

Perturbation modeling has the advantage of a more direct interpretation of results than when using more complex models involving a multitude of physical processes and interactions. For example, to evaluate how the accumulation regions of ice sheets may respond to changes in accumulation rate and temperature, *Whillans* [1981] considers perturbations to the lamellar flow solution. This analysis allows the effect of climate variations on the depth-age and depth-temperature profiles to be calculated. *Cuffey and Clow* [1997] use a purely diffusive approximation to compute changes in ice divide thickness and to estimate a time scale for response to climate forcing. *Nereson et al.* [1998] use a model based on linearized perturbations about a two-dimensional Vialov-Nye ice sheet profile to investigate the sensitivity of the divide position at Siple Dome, West Antarctica, to small changes in the accumulation pattern. These studies, and many others as well, use simple models that retain the essential physical processes to study ice sheet response to modest climate forcing.

Mass balance forcing has an immediate effect on the ice sheet. Initially, the rate of thickness change as compared to the reference state equals the perturbation in snowfall or ablation. If the forcing persists, the ice sheet responds dynamically, adjusting the rate at which ice is evacuated from the interior to the margins, to achieve a new equilibrium. For large ice sheets, this dynamic adjustment may last for thousands of years, with the magnitude of change decreasing steadily over time as a new equilibrium is approached. This response can be described using kinematic wave theory, first introduced into glaciology by *Nye* [1958] and *Weertman* [1958]. This theory, modified to pertain to Greenland drainage basins, is used here to evaluate possible ice sheet responses to perturbations in surface mass balance. The objective here is not to accurately model observed changes in ice thickness but rather to assess the range of mass imbalances that could, potentially, be attributed to changes in surface mass balance.

Implicitly, in formulating the kinematic wave model, the assumption is made that the perturbations remain sufficiently small so as not to affect the dynamics of the reference state, and rapid switches in flow style are precluded a priori from the analysis. To investigate the Jakobshavn Effect, a model that incorporates longitudinal stress gradients and other sources of flow resistance, is needed. As explained more fully below, the Jakobshavn Effect is believed to be initiated by increased calving from the floating outlet glaciers. Thus a first step in studying this instability mechanism is to assess how large calving events affect the flow upglacier and, in particular, whether such an event leads to increased stretching. This interaction is discussed here in the context of prior modeling studies as well as observations, to assess whether release of back pressure associated with major calving events is compensated entirely by longitudinal stresses, as in the model proposed by *Hughes* [1986, 1998], or whether lateral drag takes up part of the additionally required resistance to flow.

2. Kinematic Waves

2.1. Background

Changes in surface mass balance or local changes in ice thickness lead to perturbations in the ice flux and adjustments in the glacier profile [*Weertman*, 1958; *Nye*, 1958, 1960, 1963]. These adjustments are described by the kinematic wave equation [*Van der Veen*, 1999a, Section 10.2]

$$\frac{\partial H}{\partial t} = -H\frac{\partial C_o}{\partial x} - \left(C_o - \frac{\partial D_o}{\partial x}\right)\frac{\partial H}{\partial x} + D_o\frac{\partial^2 H}{\partial x^2} + M \ , \quad (1)$$

In this expression, H represents the perturbation in ice thickness, M is the change in surface mass balance, and x denotes the curvilinear along-flow direction. Equation (1) is derived by linearizing the perturbation flux Q using a series expansion

$$Q = \left(\frac{\partial Q}{\partial H}\right)_o H + \left(\frac{\partial Q}{\partial \alpha}\right)_o \alpha = C_o H + D_o \alpha \ , \quad (2)$$

and substitution in the continuity equation expressing conservation of mass (or volume, if the density is considered constant). In (2) the subscript o refers to the reference state, and α represents the surface slope (taken positive when the surface elevation decreases in the direction of flow).

Assuming lamellar flow, the coefficients C_o and D_o, which represent the sensitivity of the ice flux to changes in ice thickness and surface slope, respectively, are given by

$$C_o = \left(\frac{\partial Q}{\partial H}\right)_o = (n+2)U_o \ , \quad (3)$$

$$D_o = \left(\frac{\partial Q}{\partial \alpha}\right)_o = \frac{nQ_o}{\alpha_o} \ , \quad (4)$$

where n represents the exponent in Glen's flow law, and U_o is the reference ice velocity [*Nye*, 1960; *Van der Veen*, 1999a, p. 313]. The coefficient C_o corresponds to the speed at which the kinematic wave travels downglacier, while D_o represents the diffusivity for horizontal diffusion of the perturbation. It should be noted that the assumption of lamellar flow is not a requirement for kinematic waves to occur. These waves owe their existence to conservation of volume or mass when a relation exists between discharge, ice thickness, and along-flow position. In deriving (1), no assumption about the flow regime is made other than that the perturbation flux can be linearized as in (2); assuming lamellar

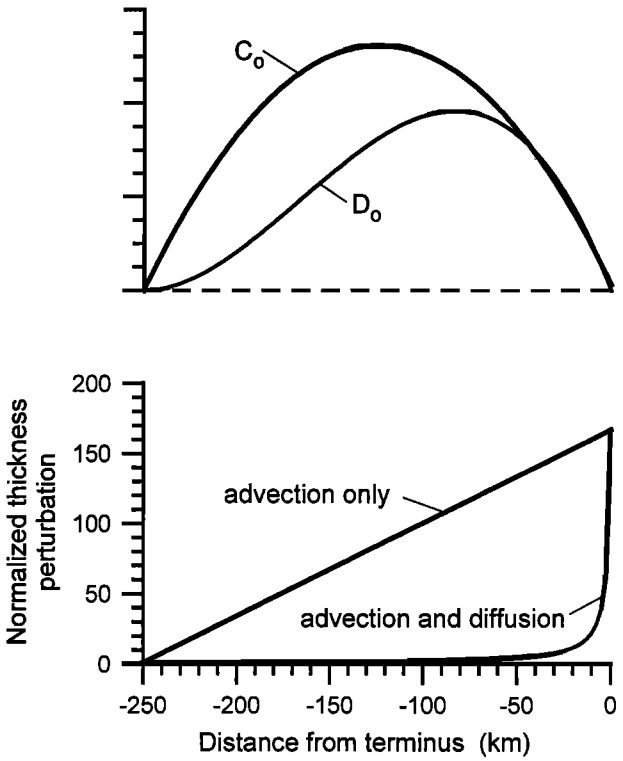

Figure 1. (top) Along-flow variation in kinematic wave velocity C_o and diffusivity D_o adopted in the Nye model and (bottom) corresponding equilibrium response after a stepwise uniform increase in surface accumulation. Thickness perturbations are normalized with the perturbation at the ice divide.

flow allows expressions for the wave speed and diffusivity to be derived. However, as argued below, (3) and (4) do not apply to Greenland outlet glaciers, and empirical relations are used in this study. The reason for introducing Nye's solution based on lamellar flow is to illustrate the differences between earlier models and the present empirical approach.

2.2. Nye's Solution

To arrive at a solution for the perturbation thickness, an assumption about the along-flow variation in C_o and D_o is needed. The usual procedure, due to *Nye* [1963], is to adopt a polynomial expression such that the glacier speed is maximum about halfway along the glacier and decreasing to zero at the glacier snout. These parameterizations are shown in the top panel of Figure 1; the bottom panel shows the equilibrium solution for the perturbation thickness after a uniform increase in surface accumulation, for the case of advection only, and for advection and diffusion.

Perhaps the most striking feature of the Nye solution is the amplification of the response toward the glacier terminus. At the edge the equilibrium change in ice thickness is about 160 times that at the divide. This large response in the lower reaches is the direct consequence of the parameterization for ice speed adopted by *Nye* [1963]. The imposed zero speed at the snout (Figure 1, top panel) effectively prevents mass from leaving the glacier and an increase in snowfall leads to piling up of mass near the terminus.

The parameterization for surface speed and the ratio of ice flux to surface slope adopted by Nye are based on velocity profiles measured along valley glaciers losing mass primarily through ablation in the terminal region. However, these functions do not apply to the polar ice sheets, where the speed increases continuously toward the grounding line and calving represents a major source of ice loss.

2.3. Empirical Relations for the Greenland Ice Sheet

While much of the margin of the Greenland ice sheet is land based and above sea level, drainage from the interior is primarily through numerous outlet glaciers whose termini are grounded below sea level or that have formed floating ice tongues in confining fjords. Considering flow lines extending from the interior to the termini of these outlet glaciers, glacier speed increases steadily as illustrated in Figure 2. The top panel shows the geometry of Petermann Glacier, based on the digital elevation

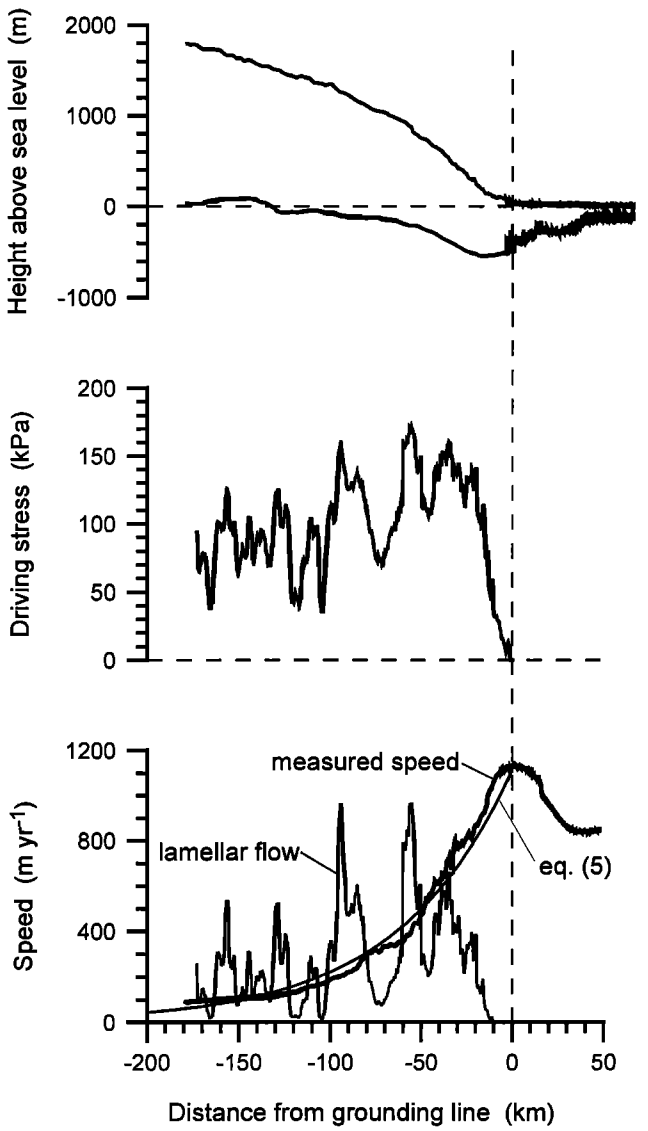

Figure 2. (top) Surface and bed elevation along the approximate centerline of Petermann Glacier, northwest Greenland. (middle) Driving stress obtained from the glacier geometry, using a horizontal distance of 10 km for calculating surface slope. (bottom) Measured surface speed and speed calculated for lamellar flow using a rate factor corresponding to ice near the pressure-melting point.

model of *Ekholm* [1996] and ice thickness data from ice-penetrating airborne radar sounding [*Gogineni et al.*, 1998]. The lower 50 km or so of this glacier is floating, confined laterally by fjord walls, and is not considered in the present analysis. Applying the familiar formula involving the product of ice thickness and surface slope (averaged over horizontal distances of ~10 km), the driving stress can be calculated (middle panel). Using a rate factor applicable to ice near the pressure-melting point, the surface speed from lamellar flow can be calculated [*Van der Veen*, 1999a, p. 104]; results for the Petermann flow line are shown in the bottom panel of Figure 2. Also shown in this panel is the surface speed derived from synthetic aperture radar interferometry (see *Joughin et al.* [1999], for the grounded portion and *Rignot* [1996] for the floating part). Up to ~40 km upglacier of the grounding line, the measured speed follows the general increase in speed from lamellar flow, suggesting that in this region, part or all of the ice flow may be associated with internal deformation. Closer to the grounding line, however, basal sliding must become the major contributor to ice discharge, as the observed velocity continues to increase toward the grounding line, while the contribution from internal deformation decreases rapidly due to the decrease in driving stress. Moreover, it could be argued that the calculated spatial fluctuations in the lamellar flow velocity indicate a more complex flow regime than assumed in that calculation. Given these observations, it is not clear how the expressions for the coefficients C_o and D_o should be modified to provide a more realistic description of the flow along this flow line. However, instead of deriving analytical expressions for these coefficients, an alternative procedure is to use the observations to derive empirical relations.

In first approximation the glacier speed shown in Figure 2 increases exponentially toward the grounding line. Taking the length of the flowband to be 500 km based on the map given by *Joughin et al.* [1999], and requiring the speed to be zero at the divide, the following parameterization is adopted:

$$U_o = 1115 \cdot e^{x/62} - 0.345 \quad \text{m yr}^{-1} , \tag{5}$$

with $x = 0$ at the grounding line and $x = -500$ km at the ice divide. As in Nye's analysis, the kinematic wave speed C_o is assumed to be proportional to U_o, with the constant of proportionality equal to 5 (the precise value of this constant has little effect on the results discussed below).

An expression for the diffusivity can be found by considering the relation between the reference ice flux and surface slope. The reference ice flux was obtained from the ice thickness and measured surface velocity by multiplying the latter with a correction factor (= 4/5) where lamellar flow contributes mostly to ice discharge (that is, at distances greater than ~40 km from the grounding line; Figure 2) to account for depth variation in ice velocity. Bivariate regression suggests a linear relation between these two quantities:

$$Q_o = 30.24 \times 10^6 \alpha_o + 22.44 \times 10^3 . \tag{6}$$

Applying this empirical relation suggests a constant diffusivity,

$$D_o = \left(\frac{\partial Q}{\partial \alpha} \right)_o = 30.24 \times 10^6 \ \text{m}^2 \ \text{yr}^{-1} . \tag{7}$$

2.4. Including Variable Width

In the original analysis presented by *Nye* [1963] the width of the glacier was considered constant. This restriction can be relaxed by considering the equation of continuity for a flowband of variable width [*Van der Veen*, 1999a, p. 332]. Transverse variations in glacier speed are neglected and the lateral margins of the drainage basin are assumed to be vertical. Adopting the parameterizations for wave speed and diffusivity discussed above, the resulting equation describing the ice sheet response to perturbations in surface mass balance is

$$\frac{\partial H}{\partial t} = -\frac{1}{W} \frac{\partial}{\partial x} \left[5 H W U_o - W D_o \frac{\partial H}{\partial x} \right] + M , \tag{8}$$

in which W represents the half width of the flowband.

The first term between the brackets on the right-hand side of the wave equation (8) describes adjustment of the glacier profile by advection, while the second term describes how local perturbations are diffused along the glacier. For the case of diffusion only, an analytical solution can be derived but otherwise, (8) is solved for prescribed width and mass balance forcing using a fully explicit, forward in time, finite difference numerical model with 5 km horizontal grid spacing and a time step of 0.1 year (to keep the solution stable).

3. Response to Grounding Line Forcing

3.1. Background

Imposed thinning at the grounding line represents a local forcing that is attenuated along the glacier primarily through diffusion [*Alley and Whillans*, 1984]. Assuming constant width for now, the kinematic wave equation (8) simplifies to

$$\frac{\partial H}{\partial t} = D_o \frac{\partial^2 H}{\partial x^2} . \tag{9}$$

Keeping the position of the grounding line fixed, a solution can be found following the procedure outlined by *Turcotte and Schubert* [1982, section 4.15] for instantaneous heating or cooling of a semi-infinite half-space.

3.2. Solution

Rather than considering thickness perturbations, it is convenient to introduce the non-dimensional quantity

$$\hat{H} = \frac{H(x,t)}{H(0,t)} , \tag{10}$$

in which the denominator represents the prescribed thickness change at the grounding line. The next step is to define the similarity variable

$$\eta = \frac{x}{2\sqrt{D_o t}} . \tag{11}$$

Using formal similarity theory, it can be shown that the solution, $\hat{H}(x,t)$, is a function of η only.

Rewriting the derivatives in the diffusion equation in terms of η gives [*Turcotte and Schubert*, 1982, p. 159]

$$-\eta \frac{d\hat{H}}{d\eta} = \frac{1}{2} \frac{d^2 \hat{H}}{d\eta^2} . \tag{12}$$

Defining

$$\Phi = \frac{d\hat{H}}{d\eta} , \tag{13}$$

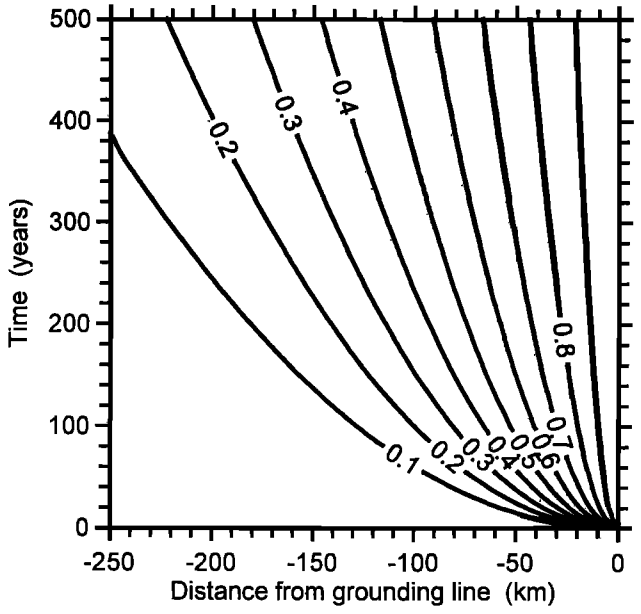

Figure 3. Transient glacier response to a sudden thinning at the grounding line at time $t = 0$ year. Contours represent the thickness perturbation normalized by the imposed change at the grounding line.

and substitution in (12) gives

$$-\eta\Phi = \frac{1}{2}\frac{d\Phi}{d\eta} , \tag{14}$$

which can be integrated to give

$$\Phi = C_1 e^{-\eta^2} = \frac{d\hat{H}}{d\eta} . \tag{15}$$

One further integration gives the nondimensionalized thickness perturbation

$$\hat{H}(\eta) = C_1 \int_0^{\eta} e^{-\bar{\eta}^2} d\bar{\eta} + C_2 . \tag{16}$$

The integration constants can be determined from the boundary conditions. At the grounding line, $\eta = 0$ and $\hat{H} = 1$ by definition, giving $C_2 = 1$. At $t = 0$, $\eta \to \infty$ and the thickness perturbation should be zero except at the grounding line. In other words, an instantaneous ice sheet response to grounding line forcing is prohibited. Note that $\eta \to \infty$ also applies at all times at distances far inland ($x \to \infty$), so this boundary condition implies that the thickness perturbation decreases toward the interior and vanishes sufficiently far inland from the grounding line. Using

$$\int_0^{\infty} e^{-\bar{\eta}^2} d\bar{\eta} = \frac{\sqrt{\pi}}{2} , \tag{17}$$

the other integration constant C_1 is found to be equal to $-2/\sqrt{\pi}$.

The solution can now be written as

$$\hat{H}(\eta) = 1 - \frac{2}{\sqrt{\pi}} \int_0^{\eta} e^{-\bar{\eta}^2} d\bar{\eta} = 1 - \mathrm{erf}(\eta) = \mathrm{erfc}(\eta) , \tag{18}$$

with $\mathrm{erf}(\eta)$ the error function and $\mathrm{erfc}(\eta)$ the complementary error function. Values for these functions can be found in mathematical handbooks or calculated using standard numerical routines [e.g., *Press et al.*, 1992, pp. 213-214].

3.3. Results

Figure 3 shows a wave of adjustment traveling upglacier after a sudden change in thickness at the grounding line at $t = 0$ years. At distances greater than about 100 km from the grounding line, the response lags considerably behind the forcing. This is better illustrated in Figure 4, which gives the perturbation in ice thickness, normalized with the imposed change at the grounding line (Figure 4a), and the time needed for partial adjustment to occur along the glacier (Figure 4b). The slow response results from the assumption that diffusion is the controlling process for adjustment. For a diffusion equation such as (9), a time L^2/D_o is required for thickness perturbations to propagate upglacier over a distance L. With $D_o = 30.24 \times 10^6$ m^2 yr^{-1}, about 330 years are required for the perturbation to travel 100 km inland. Because the timescale for adjustment is proportional to the square of distance from the grounding line, the speed at which the wave propagates inland decreases rapidly toward the interior. Near the grounding line, this speed is ~30 km yr^{-1} but at 100 km inland, the wave speed has decreased to ~300 m yr^{-1}.

The diffusive response to grounding line forcing is associated with upglacier attenuation of perturbations in surface slope. Only the slope effect (second term on the right-hand side of (2)) on the perturbation flux is retained. Consequently, the results in Figures 3 and 4 do not include possible feedbacks associated with the Ja-

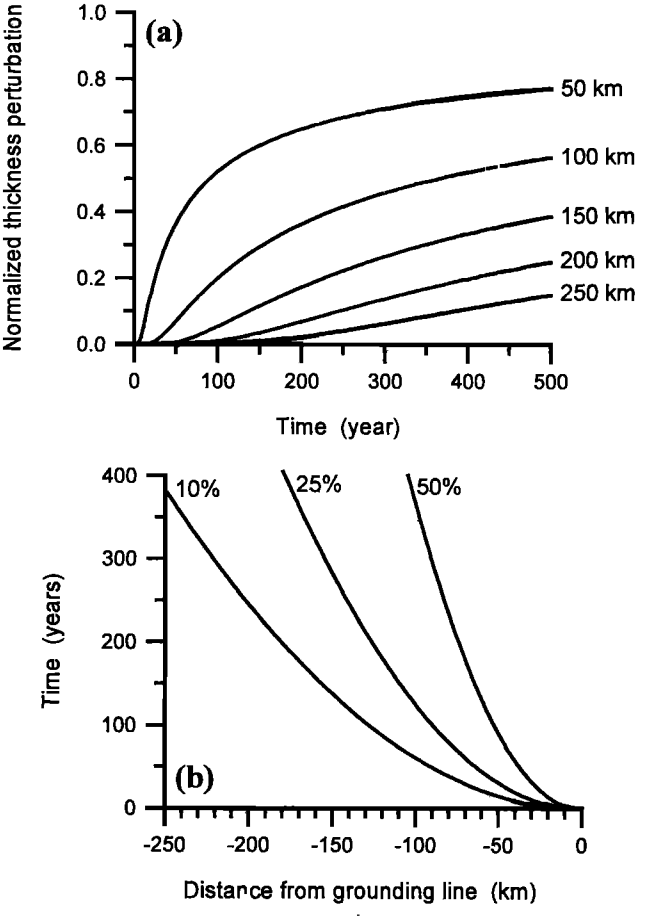

Figure 4. (a) Normalized thickness perturbation at selected distances upstream of the grounding line and (b) time required for partial adjustment (labels indicate the amount of adjustment as a fraction of the equilibrium response) following sudden grounding line thinning at time $t = 0$ year.

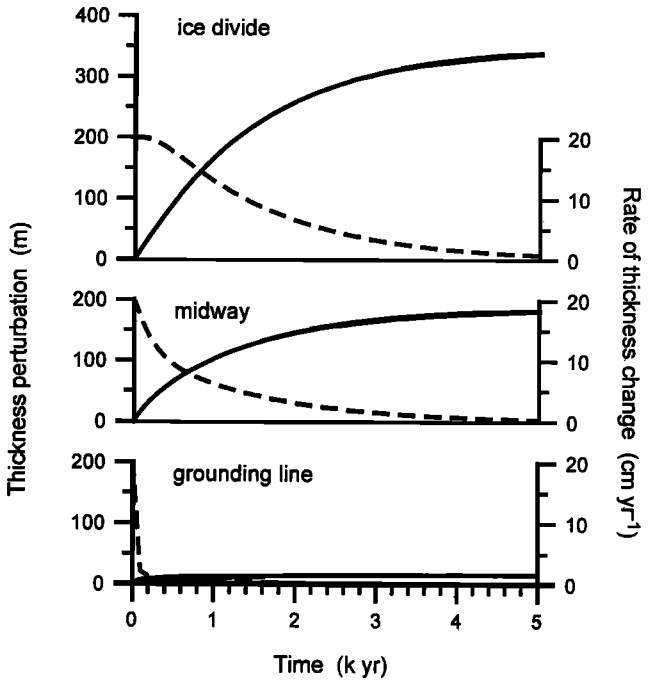

Figure 5. Ice sheet response to a uniform increase in surface accumulation ($M = 0.20$ m yr^{-1}). Constant width is assumed. The solid curves (scale on the left) show the thickness perturbation, and the dashed curves (scale on the right) show the rate of thickness change at three points on the glacier.

kobshavn effect [*Hughes*, 1986]. According to Hughes' model, thinning at the grounding line may lead to greater stretching rates in the interior, resulting in increased ice discharge, enhancing the thinning at the grounding line. This positive feedback is not included in the kinematic wave model because the reference velocity U_a is considered constant with time.

4. Response to Accumulation Forcing

4.1. Constant Width

To evaluate the response to changes in accumulation, the full continuity equation (8) for thickness perturbations needs to be integrated forward in time using standard numerical solution techniques. To allow for a comparison with Nye's solution, consider first the response of a glacier of constant width to a uniform perturbation in surface accumulation. A uniform increase in accumulation of 0.20 m yr^{-1} is imposed at time $t = 0$ year, and the kinematic wave equation (8) integrated forward in time to determine the transient glacier response. Results of this calculation are shown in Figures 5 and 6.

Figure 5 shows the response at three points along the glacier, the ice divide and the grounding line, and the grid point halfway in between. The full curves (scale on the left) give the perturbation thickness and the dashed curves (scale on the right) the rate of adjustment. The glacier responds immediately to the increased snowfall, initially thickening at a rate equal to the perturbation in accumulation. At the grounding line the rate of thickness change decreases rapidly and a new equilibrium is established after a few hundred years. Farther upglacier, adjustment takes longer, up to about 5000 years at the divide. Figure 6 shows contour plots of the adjustment along the entire flow line. From these graphs the equilibrium response can be inferred. The most striking feature of the new equilibrium is that the response is greatest at the ice divide and decreases toward the grounding line.

For a uniform change in surface mass balance, the equilibrium response along the entire glacier, normalized with the thickness change at the divide, is as shown in Figure 7. The amplitude of the perturbation decreases toward the grounding line, where the response is about 5% of that at the divide. This finding is oppo-

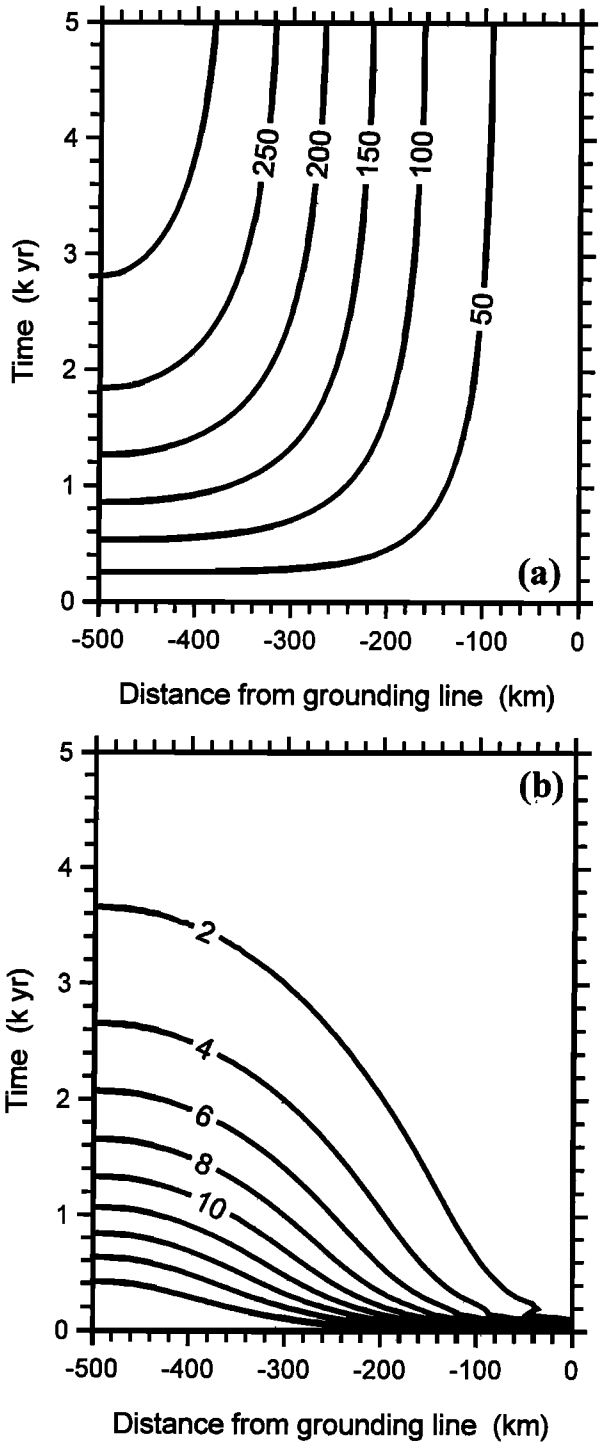

Figure 6. Transient glacier response to a sudden increase in surface accumulation at time $t = 0$ year. (a) Thickness perturbation (contour interval 50 m) and (b) rate of thickness change (contour interval 2 cm yr^{-1}).

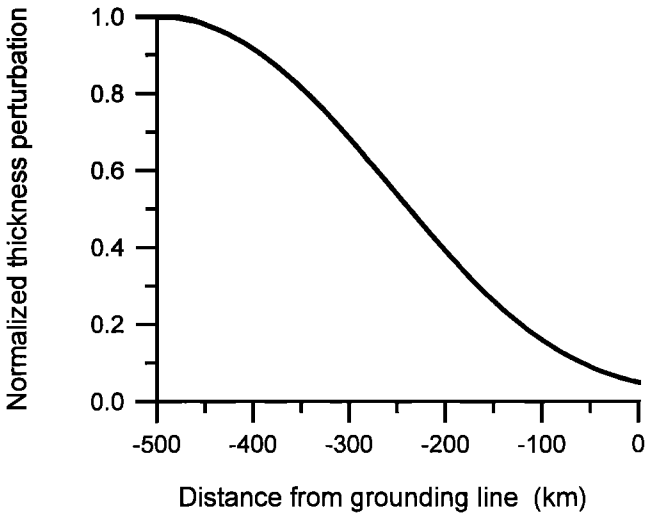

Figure 7. Normalized equilibrium response after a stepwise uniform increase in surface accumulation, assuming constant width for the flowband.

site to the result derived by *Nye* [1963] which shows the greatest response at the glacier terminus (Figure 1). As noted above, the amplification of thickness change near the glacier snout is the result of the parameterization of glacier speed adopted by Nye, which does not permit mass to leave the glacier. Adopting a velocity profile more realistic for polar drainage basins, with speed increasing steadily toward the grounding line, part of the increase in surface accumulation is evacuated across the grounding line.

4.2. Variable Width

The top panel in Figure 8 shows the width of the Petermann flowband. Accounting for the change in width along the flow line affects the equilibrium solution twofold. First, the response at the divide is about 30% less than if a constant width is prescribed. Otherwise, the equilibrium response is similar, with the amplitude decreasing away from the divide, as shown in the bottom panel of Figure 8. Approaching the grounding line, the equilibrium thickness change increases as ice is being funneled into the narrow outlet fjord. Compared to the constant-width case, a greater amount of snow accumulating in the wider catchment region must be evacuated across the grounding line through the narrow discharge gate. This is achieved by increasing the perturbation flux by increasing the perturbation thickness and surface slope.

4.3. Nonuniform Mass Balance Forcing

Imposing a uniform change in surface mass balance, as in the examples shown in Figures 5-8, allows the results of the present model to be compared with those obtained in earlier studies. However, a uniform forcing may not be realistic. In the context of global warming, it is generally believed that accumulation may increase in the interior, but surface melting is expected to increase considerably at lower elevations. Prescribing a logistic variation for the mass balance perturbation,

$$M = \frac{M_o}{1 + \gamma e^{-\beta x}} - M_1 , \qquad (19)$$

allows a smooth transition in forcing from the interior to the terminus region. Two parameterizations used to force the kinematic

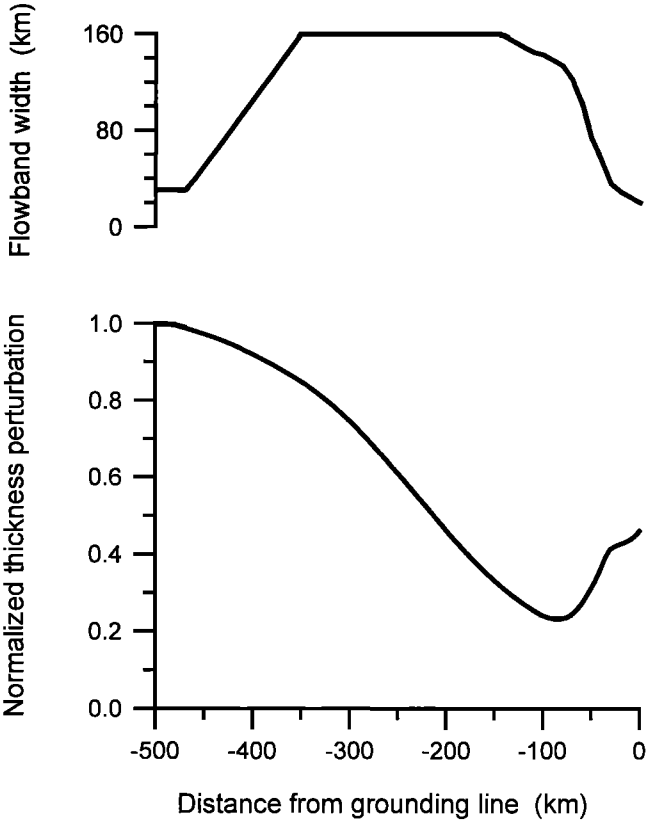

Figure 8. Normalized equilibrium response after a stepwise uniform increase in surface accumulation and accounting for the width of the flowband (shown in the top panel).

wave model are shown in Figure 9. The corresponding glacier responses are shown in Figures 10 and 11.

Of particular interest is the glacier's response in the terminal region. Initially, imposed ablation leads to rapid thinning, but after a few hundred years this trend is reversed and the glacier snout starts thickening. For the case of increased snowfall in the interior (Figure 10), the thickening rate reaches a few centimeters per year after 200 years and decreases steadily after that. As a re-

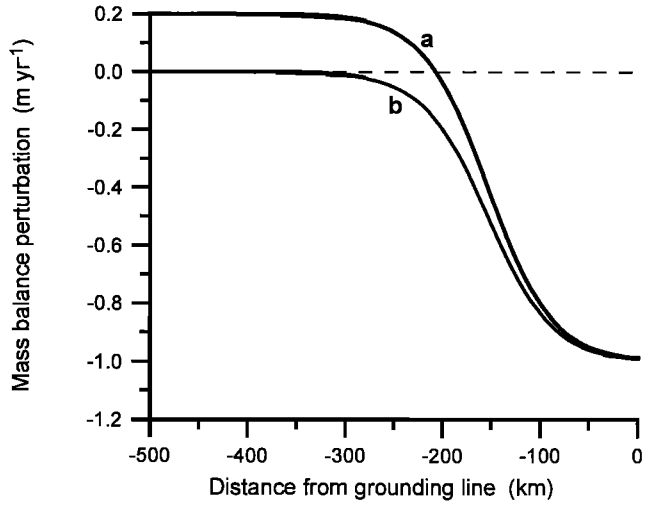

Figure 9. Two mass balance perturbations used as forcing for the present model.

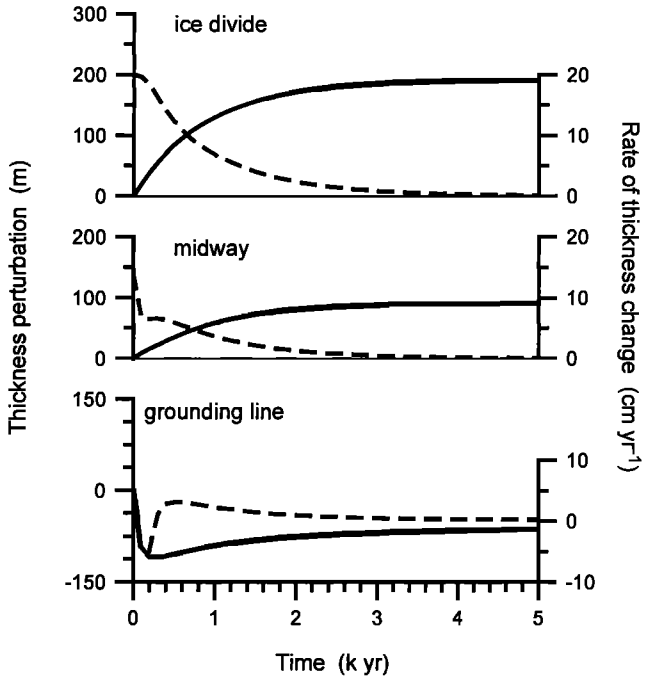

Figure 10. Ice sheet response to the accumulation perturbation shown in Figure 9 (curve a). The solid curves (scale on the left) show the thickness perturbation, and the dashed curves (scale on the right) show the rate of thickness change at three points on the glacier.

sult, after a new equilibrium is reached, the thickness at the grounding line is not much different from the reference state. That is, the perturbation thickness is near zero, despite the large increase in ablation. The increase in accumulation at higher elevations more than compensates for the mass loss at lower elevations, which is restricted to a smaller area. If ablation is not compensated by more snowfall in the interior (Figure 11), a wave of thinning travels upglacier such that the maximum rate of thickness change occurs at the grounding line first, reaching the ice divide after about 600 years. Similar manifestations of the delayed dynamical response to changes in surface mass balance have been found using more complex numerical ice sheet models [e.g., *Oerlemans*, 1982].

5. Jakobshavn Effect

5.1. Background

Krabill et al. [1999] suggest that the large thinning rates on outlet glaciers may be associated with enhanced creep rates, possibly due to lowered basal friction as surface meltwater reaches the glacier bed. A similar set of positive feedback mechanisms was proposed by *Hughes* [1986] and termed the Jakobshavn Effect. In essence, this effect acts to amplify a small initial perturbation, resulting in large changes in glacier discharge. *Hughes* [1998] argues that the Jakobshavn Effect may have been an important factor in the collapse of paleo ice sheets that disappeared rapidly starting around 18 kyr B.P. and may lead to rapid disintegration of the present-day Greenland and Antarctic ice sheets.

The trigger for the Jakobshavn Effect is surface melting. Because the surface of many outlet glaciers is heavily crevassed, the greater exposed surface area allows more solar radiation to be absorbed than if the surface were smooth, resulting in vast amounts of surface meltwater that drains into the glacier. If meltwater refreezes at depth, the release of latent heat warms the ice and thus increases the rate of deformation. Water that reaches the glacier base provides lubrication, allowing more rapid glacier sliding. Both effects lead to greater ice speeds, which promotes further surface crevassing thereby further increasing the exposed surface area. On the floating parts of outlet glaciers, thinning reduces resistance to flow from bedrock pinning points and lateral drag, and the buttressing effect on the grounded portion decreases, allowing further increase in ice discharge. Moreover, thinning on the floating ice tongue may lead to increased iceberg calving as the vertical thickness that needs to be fractured becomes less. Increased calving leads to retreat of the glacier front and reduces the backstress exerted on the inland ice. This aggregate of physical processes acts to lessen mechanical constraints imposed on the grounded lower regions of the outlet glaciers, leading to rapid increase in ice discharge.

5.2. Cause of Instability

Considering a floating ice tongue or ice shelf, resistance to flow is partitioned between gradients in longitudinal stress and lateral drag. Averaged over the width of the glacier, force balance is then expressed through [*Thomas*, 1973; *Sanderson*, 1979; *Van der Veen*, 1986; *Van der Veen*, 1999a, p. 130]

$$\tau_{dx} = -\frac{\partial}{\partial x}\left[H R_{xx}\right] + \frac{H \tau_s}{W} . \qquad (20)$$

In deriving this balance equation the assumption is made that lateral drag is equally important across the width of the glacier. Lateral stress at the margins, $y = \pm W$ is denoted by τ_s. The partitioning of full stresses into lithostatic and resistive components [*Van der Veen and Whillans*, 1989] is used here, and R_{xx} represents the along-flow or longitudinal resistive stress. If lateral spreading and bridging effects are neglected, this stress equals twice the longitudinal deviatoric stress ($R_{xx} = 2\sigma'_{xx}$) [*Van der Veen and Whillans*, 1989; *Van der Veen*, 1999a, p. 38].

The left-hand side of (20) represents the driving stress. For a floating glacier the elevation of the surface above sea level is linked to the ice thickness, H, through hydrostatic equilibrium, and the driving stress can be written as [*Van der Veen*, 1999a, p. 128]

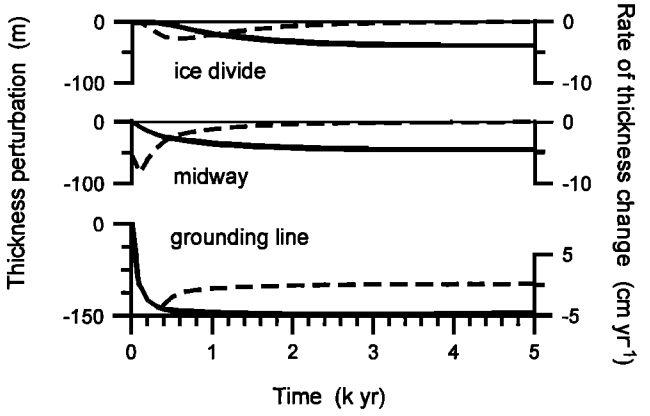

Figure 11. Ice sheet response to the accumulation perturbation shown in Figure 9 (curve b). The solid curves (scale on the left) show the thickness perturbation, and the dashed curves (scale on the right) show the rate of thickness change at three points on the glacier.

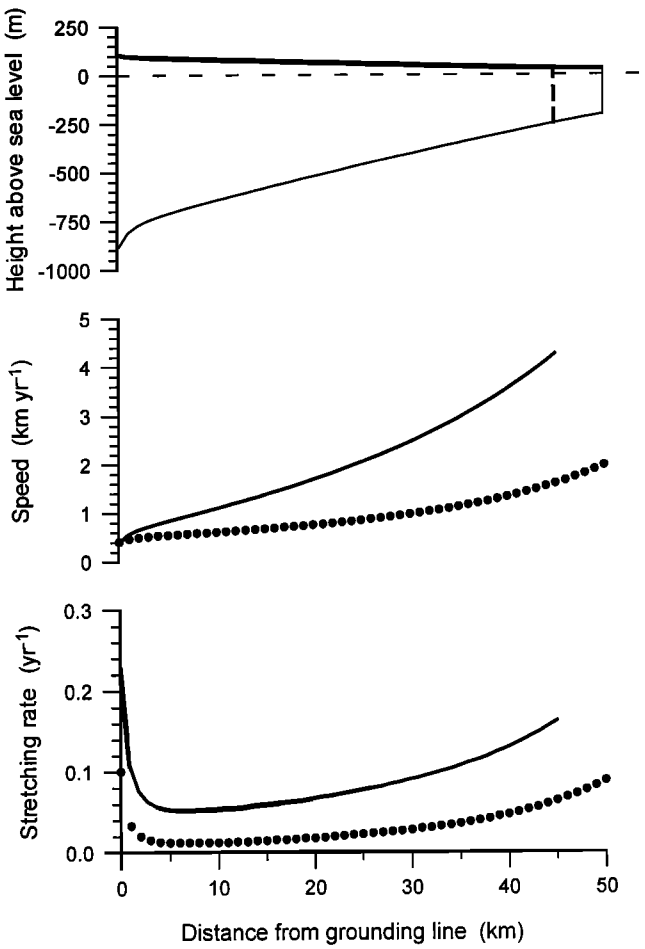

Figure 12. Effect of a calving event on the speed and stretching rate along an ice shelf of constant width and with prescribed and fixed shear stress at the lateral margins. (top) The equilibrium profile is shown and the vertical dashed line indicates the reduction in glacier length. (middle, bottom) The dotted curves correspond to the equilibrium speed and stretching rate prior to calving, while the solid curves show speed and stretching rate after calving.

$$\tau_{dx} = -\frac{1}{2}\left[1 - \frac{\rho}{\rho_w}\right]\frac{\partial H^2}{\partial x} , \qquad (21)$$

where ρ and ρ_w are the densities of ice and seawater, respectively.

The first term on the right-hand side of the balance equation (20) describes resistance to flow offered by gradients in longitudinal stress. The along-flow resistive stress R_{xx} is linked to the stretching rate, or gradient in discharge velocity, through the flow law for glacier ice. If lateral drag contributes negligibly to flow resistance the second term on the right-hand side of (20) may be neglected. Substituting (21) for the driving stress into the balance equation (20) and integrating with respect to the along-flow direction x the resistive stress is found to be proportional to the ice thickness [*Weertman*, 1958; *Van der Veen*, 1999a, p. 128]

$$R_{xx}^{(o)} = \frac{1}{2}\rho g\left[1 - \frac{\rho}{\rho_w}\right]H . \qquad (22)$$

Invoking the flow law gives the stretching rate

$$\dot{\varepsilon}_{xx}^{(o)} = \left[\frac{\rho g}{4B}\left(1 - \frac{\rho}{\rho_w}\right)\right]^3 H^3 , \qquad (23)$$

in which B represents the rate factor in Glen's flow law, and the flow law exponent has been set equal to 3. The superscript *(o)* in these expressions is used to differentiate this solution, applicable to an ice tongue spreading in one direction only with little or no lateral drag, to the solution for the case of significant lateral drag.

If lateral drag contributes to resistance to flow, the stretching stress at any point along the ice tongue $R_{xx}(x)$ is reduced compared to the Weertman solution (22) by an amount equal to the integrated resistance from lateral drag acting on the segment of glacier from that point to the calving front. In short,

$$R_{xx}(x) = R_{xx}^{(o)}(x) - \sigma_b(x) , \qquad (24)$$

in which the back pressure is defined as

$$\sigma_b(x) = \frac{1}{H}\int_x^L \frac{H\tau_s}{W}\,d\bar{x} , \qquad (25)$$

with $x = L$ denoting the position of the calving front [*Thomas*, 1973; *Van der Veen*, 1999a, p. 130]. Because the stretching rate is proportional to the third power of the stretching stress, the effect of lateral drag, or back pressure, is to reduce the stretching rate according to

$$\dot{\varepsilon}_{xx}(x) = \left[\frac{R_{xx}^{(o)}(x) - \sigma_b(x)}{B}\right]^3 . \qquad (26)$$

In Hughes' model the value of the lateral shear stress at the margins τ_s is prescribed and kept constant at, say, 100 kPa. In that case, any reduction in length results in an immediate increase in stretching along the entire ice tongue. This effect is illustrated in Figure 12 which shows the speed and stretching rate along an ice shelf before (dots) and after (solid lines) a calving event. The top panel shows the equilibrium profile of an ice shelf in a parallel-sided bay (width = 40 km) calculated using a numerical model [*Van der Veen*, 1999a, section 8.8] with prescribed flux across the grounding line (H_o = 1000 m; U_o = 400 m yr^{-1}) and fixed lateral shear stress at the margins (τ_s = 150 kPa). The length of the floating glacier is restricted to 50 km, but imposing this condition has no effect on the upglacier equilibrium profile. In equilibrium the glacier speed at the terminus is slightly greater than 1 km yr^{-1}. The effect of a calving event in which the length of the glacier is reduced by 5 km (10%) is dramatic: the stretching rate at the grounding line more than doubles instantaneously and the speed at the new terminus position is in excess of 4 km yr^{-1}. This adjustment to a major calving event is the direct consequence of keeping resistance to flow from lateral drag constant by prescribing the value of τ_s. Under this assumption the back pressure on a glacier of constant width is approximately

$$\sigma_b(x) = \frac{\tau_s}{W}(L - x) . \qquad (27)$$

For the example shown in Figure 12, the back pressure at the grounding line is 375 kPa, compared to a free-floating stretching stress of 485 kPa (from (22)). Thus the net longitudinal resistive stress is only 10 kPa at the grounding line. Reducing the glacier length by 10% reduces σ_b at the grounding line by 38 kPa,

thereby increasing the longitudinal resistive stress to 48 kPa, almost 5 times as large as before the calving event.

5.3. Stabilizing Effects

While a major calving event may have some effect on the stretching rate immediately upglacier of the calving front, it appears unlikely that the reduction in back pressure along the entire glacier is compensated for by an increase in longitudinal stress gradients. The consequent increase in speed shown in the middle panel of Figure 12 almost surely would increase lateral drag and hence lower the stretching rate. In other words, one may expect that the effects of reduced back pressure due to shortening of the glacier will be in part mitigated by increased lateral drag. To investigate this point, lateral drag needs to be linked to glacier discharge.

Following the ice stream model developed by *Van der Veen and Whillans* [1996], the shear stress at the margins can be written in terms of the width-averaged speed as

$$\tau_s = B\left(\frac{5}{2}\frac{U}{W}\right)^{1/3}. \tag{28}$$

Substituting this expression into the balance equation (20) and rewriting the longitudinal resistive stress R_{xx} in terms of the along-flow gradient in ice velocity, yields an equation with the glacier speed U as only unknown. However, this equation is nonlinear and contains gradients and cannot be solved directly and, instead, numerical iteration techniques must be used. Several numerical schemes were implemented, but none turned out to be stable, and further attempts to use a numerical ice shelf model to evaluate the response to a calving event were abandoned. Nevertheless, based on the equations discussed above, a few qualitative comments can be made.

For the model ice shelf shown in Figure 12 applying (28) to the terminus region prior to the calving event gives τ_s = 152 kPa, close to the constant value prescribed in the numerical calculation. Assuming that, following the calving event, τ_s increases by 10% along the entire length of the ice shelf, increased resistance from lateral drag leads to an increase in back pressure at the grounding line of (15 kPa × 45 km) / 20 km = 33 kPa, which is almost the same as the reduction in σ_b due to the reduction in ice shelf length. A 10% increase in τ_s corresponds to approximately 30% increase in glacier speed (equation (28)). However, if resistance from lateral drag compensates for the loss of back pressure due to shortening of the ice shelf, σ_b in (26) is unaffected by the calving event implying that the stretching rate must remain the same. This would imply unchanged gradients in ice velocity and thus no change in the velocity itself. Thus the increase in glacier speed must be less, perhaps 15% or so, to allow the decrease in back pressure from calving to be distributed between lateral drag and longitudinal stress gradients. The precise percentage may depend on other factors such as softening of the ice in the lateral shear margins due to fabric orientation or strain heating, but the point made here is that lateral drag may be expected to accommodate some of the decrease in back pressure.

From this rough estimate it may be concluded that a major calving event may lead to a moderate speed up of the floating ice tongue, but the increase in speed is an order of magnitude smaller than if changes in lateral shear stress at the margins are not taken into account. Whether or not the resulting increase in speed and consequent stretching rate is sufficient to lead to further and more calving is not obvious. Observational evidence does not favor a strong correlation between the rate of iceberg production and stretching near the terminus [*Van der Veen*, 1996] although one would expect a greater stretching stress (associated with increased stretching rate) to facilitate full-thickness fracturing [*Van der Veen*, 1998]. At this stage of understanding a realistic calving law cannot be formulated but it may be noted that no Greenland outlet glaciers have been observed to retreat irrevocably after a major calving event. However, even if the calving front were to retreat to the grounding line, it is not immediately obvious that the associated lowering of back pressure would result in a collapse of the interior parts of the ice sheet.

5.4. Discussion

The Jakobshavn Effect as proposed by *Hughes* [1986] may be challenged. Calving rates on Jakobshavn Glacier increase rapidly in spring, presumably because surface meltwater penetration or break up of confining sea ice in the fjord facilitate crevasse penetration and fracturing [*Sohn et al.*, 1998]. Yet despite the almost sixfold increase in calving rate, and subsequent retreat of the floating terminus, there is no discernable seasonal fluctuation in glacier speed either on the floating portion nor farther inland on the grounded part at and below the equilibrium line [*Echelmeyer and Harrison*, 1990]. Thus, while surface melting appears to have a significant effect on calving rates, the supposed effect on discharge from the interior is not supported by observations. Either the seasonal fluctuations in terminus position are not sufficiently large or the buttressing effect has a significantly smaller effect on drainage from the interior than envisioned by Hughes.

A number of model studies has addressed the issue of grounding line stability in response to reduction in ice shelf back pressure or sea level rise, and all suggest that enhanced creep thinning at the grounding line is rapidly countered by increased discharge from upglacier, effectively preventing the collapse of model ice sheets. *Alley and Whillans* [1984] use a nonsteady ice flow model that includes longitudinal stresses explicitly to study the stability of the East Antarctic ice sheet to sea level rise. Imposing a 100-m rise in sea level results in a wave of thinning propagating upglacier, but their model does not exhibit signs of flow instability. A similar model but including basal sliding was used by *Van der Veen* [1985, 1987] to investigate the stability of marine ice sheets. The ice shelf back pressure is incorporated through the longitudinal stress deviator, prescribed at the grounding line. Model results suggest greater stability to reduction in back pressure than assumed in the Jakobshavn Effect. Grounding line retreat is controlled by a number of counteracting processes of which the relative importance cannot be established a priori. In particular, enhanced creep thinning at the grounding line due to reduced back stress is countered by increased ice discharge from upglacier. *Alley et al.* [1987] use a model coupling ice flow to deformation of subglacial till to study the stability of an ice stream moving over soft basal material. Their model indicates that the system responds rapidly but in a stable manner to imposed perturbations at the grounding line.

It appears, then, that there is little observational or modeling support for the Jakobshavn Effect as proposed by *Hughes* [1986, 1998]. That is, reducing the back pressure at the grounding line does not necessarily lead to enhanced creep thinning and instability of the grounded portion of outlet glaciers. This does not imply, however, that Greenland outlet glaciers cannot undergo rapid change. As the mass balance studies referred to earlier indicate, parts of the Greenland ice sheet may be undergoing important, albeit possibly short lived, changes. Many model studies

indicate that changes in basal conditions may alter the flow regime and greatly increase ice discharge velocities with consequent thinning.

6. Discussion

Kinematic wave theory provides an expedient tool for studying the response of glaciers and ice sheets to climate forcing. Because perturbations on a reference state are considered, the particulars of the dynamical flow regime of the ice sheet (such as sliding relation, partitioning of flow resistance, etc.) need not be explicitly known. Rather, these are incorporated through the parameterization of the reference ice flux or longitudinal velocity profile. In this study, surface speeds measured along Petermann Glacier are used to account for the dynamics of the ice sheet, but other profiles could be used to reflect different flow regimes. The resulting equation for the time evolution of thickness perturbations is readily solved numerically without the need for large CPU time.

In the present model, if constant width is assumed for the flowband, the greatest response to uniform accumulation forcing is found at the divide. Near the glacier terminus or grounding line, the perturbation thickness is smallest, due to the advection of excess mass across the grounding line. Incorporating the variable width of the drainage basin, and in particular the funneling of ice into the outlet fjord, results in an amplification of the response in the lower reaches. In all cases the timescale of adjustment is of the order of a thousand years or so.

Adjustment of ice discharge to altered surface accumulation becomes important soon after imposing the perturbation. The rate of thickness change is greatest immediately after changing the surface mass balance but decreases rapidly over the course of the next few centuries. *Krabill et al.* [1999] find that interior parts of southern Greenland are thickening by more than 10 cm yr^{-1}, while eastern outlet glaciers appear to be thinning at rates exceeding 1 m yr^{-1}. Such rates could be explained as resulting from a mass balance forcing similar to profile a in Figure 9, which would imply a very recent and substantial increase in snowfall in the interior and enhanced ablation near the coast. There are, however, no supporting data to corroborate this possibility, and, in fact, model studies of recent changes in precipitation over the ice sheet suggest a decrease in annual snowfall [*Bromwich et al.*, 1998]. Nevertheless, assuming the current pattern of thickness change is in response to recent changes in surface mass balance, the model results presented here indicate that the rates of adjustment, in particular the large thinning rates near the coast, should decrease markedly over the next few decades.

The major shortcoming of the kinematic wave approach is the decoupling of perturbations in ice flow from the reference state. That is, the dynamics of the reference state are assumed to remain the same. To evaluate the glacier's response to major changes at its perimeter, more complex time-evolving models that include calculation of all relevant stresses controlling ice discharge are needed.

A number of authors have suggested that reduction in back pressure exterted by a floating ice shelf or ice tongue may lead to increased discharge from the interior [*Bentley*, 1984; *Hughes*, 1986, 1998; *Mercer*, 1968, 1978; *Thomas*, 1979; *Thomas and Bentley*, 1978; *Thomas et al.*, 1979; *Weertman*, 1974). While most of these studies apply to the marine-based West Antarctic ice sheet, *Hughes* [1986] argues that a similar instability mechanism, which he termed the Jakobshavn Effect, may act to destabilize parts of the Greenland ice sheet. The trigger for instability according to Hughes is increased calving, possibly caused by enhanced surface melting. It is argued here that stabilizing effects not permitted in the models referred to above may slow down, or even halt completely, catastrophic collapse. First, a major calving event may not lead to substantial reduction in back pressure at the grounding line if lateral drag increases to compensate for the reduction in back pressure caused by shortening of the ice tongue. As shown, only a moderate increase in lateral drag would be required to achieve this. Considering that lateral drag may be expected to increase as the ice velocity increases, this appears a plausible stabilizing effect. Second, modeling studies do not support the grounding line instability hypothesis. Models that incorporate coupling between ice shelf and inland ice through longitudinal stress gradients suggest that ice sheets may be more stable to forcings at their grounding lines than sometimes believed, and that adjustments in drainage from the interior can for the most part compensate for grounding line effects. While complete removal of a buttressing ice shelf may result in temporary increase in discharge across the grounding line, further grounding line retreat is quickly halted by increased advection of ice from the interior.

In conclusion, if the observed thickness changes on the Greenland ice sheet are in response to changes in surface mass balance, it may be expected that the rates of thickness change will decrease over the next few years. However, since there is no supporting climatological evidence for important changes in snowfall and/or ablation (sufficiently large to lead to thickness changes of the observed magnitudes), it appears that the ice sheet is dynamically adjusting to other forcings, including perhaps internal instabilities. One suggested mechanism, the Jakobshavn Effect, is challenged here and argued to have a minor effect on glacier discharge, if any. This suggests that dynamic changes in the ice sheet have a different origin. It may be that recent changes in basal conditions under the outlet glaciers have led to an increase in glacier speed through enhanced sliding. Without further investigations, including determining if changes in speed have taken place, the causes for observed patterns of change in Greenland cannot be identified unambiguously. However, the present study indicates that two potential forcings, namely, kinematic adjustment to mass balance forcing and the Jakobshavn Effect, are unlikely causes.

Acknowledgments. Perspicacious comments and suggestions from Bob Thomas, Kurt Cuffey, and an anonymous reviewer helped improve this manuscript. This work was supported by NASA Goddard Space Flight Center under award NAG5-8632 and by the National Science Foundation under award OPP-9807521. Byrd Polar Research Center contribution C-1195.

References

Alley, R. B., and I. M. Whillans, Response of the East Antarctic Ice Sheet to sea-level rise, *J. Geophys. Res., 89*, 119-129, 1984.

Alley, R. B., D. D. Blankenship, S. T. Rooney, and C. R. Bentley, Till beneath ice stream B: 4. A coupled ice-till flow model, *J. Geophys. Res., 92*, 8931-8940, 1987.

Bentley, C. R., Some aspects of the cryosphere and its role in climatic change, in *Climate Processes and Climate Sensitivity, Geophys. Monogr. Ser.*, vol 29, edited by J. E. Hansen and T. Takahashi, pp. 207-220, AGU, Washington, D. C., 1984.

Bromwich, D. H., R. I. Cullather, Q. Chen, and B. M. Csathó, Evaluation of recent precipitation studies for the Greenland Ice Sheet, *J. Geophys. Res., 103*, 26,007-26,024, 1998.

Cuffey, K. M., and G. D. Clow, Temperature, accumulation, and ice sheet elevation in central Greenland through the last deglacial transition, *J. Geophys. Res., 102*, 26,383-26,396, 1997.

Echelmeyer, K., and W. D. Harrison, Jakobshavn Isbræ, West Greenland: Seasonal variations in velocity – or lack thereof, *J. Glaciol., 36*, 82-88, 1990.

Ekholm, S., A full coverage, high-resolution topographic model of Greenland computed from a variety of digital elevation data, *J. Geophys. Res., 101*, 21,961-21,972, 1996.

Gogineni, S., T. Chuah, C. Allen, K. Jezek, and R. K. Moore, An improved coherent radar depth sounder, *J. Glaciol., 44*, 659-669, 1998.

Hughes, T., The Jakobshavn effect, *Geophys. Res. Lett., 13*, 46-48, 1986.

Hughes, T., *Ice Sheets*, 343 pp., Oxford Univ. Press, New York, 1998.

Huybrechts, P., The present evolution of the Greenland Ice Sheet: An assessment by modelling, *Global Planet. Change, 9*, 39-51, 1994.

Huybrechts, P., A. Lettrequilly, and N. Reeh, The Greenland Ice Sheet and greenhouse warming, *Palaeogeogr. Palaeoclimatol. Palaeoecol., 89*, 399-412, 1991.

Joughin, I., S. Tulaczyk, M. Fahnestock, and R. Kwok, A mini-surge on the Ryder Glacier, Greenland, observed by satellite radar interferometry, *Science, 274*, 228-230, 1996.

Joughin, I., M. Fahnestock, R. Kwok, P. Gogineni, and C. Allen, Ice flow of Humboldt, Petermann and Ryder Gletscher, northern Greenland, *J. Glaciol., 45*, 231-241, 1999.

Krabill, W., E. Frederick, S. Manizade, C. Martin, J. Sonntag, R. Swift, R. Thomas, W. Wright, and J. Yungel, Rapid thinning of parts of the southern Greenland Ice Sheet, *Science, 283*, 1522-1524, 1999.

Mercer, J. H., Antarctic ice and Sangamon sea level, *IAHS Publ., 79*, 217-225, 1968.

Mercer, J. H., West Antarctic Ice Sheet and CO_2 greenhouse effect: A threat of disaster, *Nature, 271*, 321-325, 1978.

Nereson, N. A., R. C. A. Hindmarsh, and C. F. Raymond, Sensitivity of the divide position at Siple Dome, West Antarctica, to boundary forcing, *Ann. Glaciol., 27*, 207-214, 1998.

Nye, J. F., A theory of wave formation in glaciers, *IAHS Publ., 47*, 139-154, 1958.

Nye, J. F., The response of glaciers and ice sheets to seasonal and climatic changes, *Proc. R. Soc. London A, 256*, 559-584, 1960.

Nye, J. F., On the theory of the advance and retreat of glaciers, *Geophys. J. R. Astron. Soc., 7*, 431-456, 1963.

Oerlemans, J., Response of the Antarctic Ice Sheet to a climatic warming: A model study, *J. Clim., 2*, 1-11, 1982.

Press, W. H., B. P. Flannery, S. A. Teukolsky, and W. T. Vetterling, *Numerical Recipes: The Art of Scientific Computing, 2nd ed.*, 963 pp., Cambridge Univ. Press, New York, 1992.

Reeh, N., and O. Oleson, Velocity measurements on Daugaard-Jensen Gletscher, Scoresby Sund, east Greenland, *Ann. Glaciol., 8*, 146-150, 1986.

Rignot, E., Tidal motion, ice velocity and melt rate of Petermann Gletscher, Greenland, measured from radar interferometry, *J. Glaciol., 42*, 476-485, 1996.

Sanderson, T. J. O., Equilibrium profile of ice shelves, *J. Glaciol., 22*, 435-460, 1979.

Sohn, H.-G., K. C. Jezek, and C. J. van der Veen, Jakobshavn Glacier, West Greenland: 30 years of spaceborne observations, *Geophys. Res. Lett., 25*, 2699-2702, 1998.

Thomas, R. H., The creep of ice shelves: Theory, *J. Glaciol., 12*, 45-53, 1973.

Thomas, R. H., The dynamics of marine ice sheets, *J. Glaciol., 24*, 167-177, 1979.

Thomas, R. H., and C. R. Bentley, A model for the Holocene retreat of the West Antarctic Ice Sheet, *Quat. Res., 10*, 150-170, 1978.

Thomas, R. H., T. J. O. Sanderson, and K. E. Rose, Effect of a climatic warming on the West Antarctic Ice Sheet, *Nature, 227*, 355-358, 1979.

Thomas, R., T. Akins, B. Csatho, M. Fahnestock, P. Gogineni, C. Kim, and J. Sonntag, Mass balance of the Greenland Ice Sheet at high elevations, *Science, 289*, 426-428, 2000.

Turcotte, D. L., and G. Schubert, *Geodynamics: Application of Continuum Physics to Geological Problems*, 450 pp., John Wiley, New York, 1982.

Van der Veen, C. J., Response of a marine ice sheet to changes at the grounding line, *Quat. Res., 24*, 257-267, 1985.

Van der Veen, C. J., Numerical modelling of ice shelves and ice tongues, *Ann. Geophys., 4*, 45-54, 1986.

Van der Veen, C. J., Longitudinal stresses and basal sliding: a comparative study, in *Dynamics of the West Antarctic Ice Sheet*, edited by C. J. van der Veen and J. Oerlemans, pp. 223-248, D. Reidel, Norwell, Mass., 1987.

Van der Veen, C. J., Tidewater calving, *J. Glaciol., 42*, 375-385, 1996.

Van der Veen, C. J., Fracture mechanics approach to penetration of surface crevasses on glaciers, *Cold Reg. Sci. Techn., 27*, 31-47, 1998.

Van der Veen, C. J., *Fundamentals of Glacier Dynamics*, 462 pp., A. A. Balkema, Brookfield, Vt., 1999a.

Van der Veen, C. J., Evaluating the performance of cryospheric models, *Polar Geogr., 23*, 83-96., 1999b.

Van der Veen, C. J., and I. M. Whillans, Force budget; I, Theory and numerical methods, *J. Glaciol., 35*, 53-60, 1989.

Van der Veen, C. J., and I. M. Whillans, Model experiments on the evolution and stability of ice streams, *Ann. Glaciol., 23*, 129-137, 1996.

Weertman, J., Travelling waves on glaciers, *IAHS Publ., 47*, 162-168, 1958.

Weertman, J., Stability of the junction of an ice sheet and an ice shelf, *J. Glaciol. 13*, 3-11, 1974.

Weidick, A., Surging glaciers in Greenland: A status, *Rapp. Grønlands Geol. Unders., 140*, 106-110, 1988.

Whillans, I. M., Reaction of the accumulation zone portion of glaciers to climatic change, *J. Geophys. Res., 86*, 4274-4282, 1981.

C. J. van der Veen, Byrd Polar Research Center and Department of Geography, Ohio State University, 108 Scott Hall, 1090 Carmack Road, Columbus, OH 43210. (e-mail: vanderveen.1@osu.edu)

(Received July 26, 2000; revised November 29, 2000;
accepted December 11, 2000).